

Theory of the Fabry-Perot quantum Hall interferometer

Bertrand I. Halperin,¹ Ady Stern,² Izhar Neder,¹ and Bernd Rosenow³

¹*Physics Department, Harvard University, Cambridge MA 02138, USA*

²*Department of Condensed Matter Physics, Weizmann Institute of Science, Rehovot 76100, Israel*

³*Institute for Theoretical Physics, Leipzig University, D-04009 Leipzig, Germany*

(Dated: September 4, 2018)

We analyze interference phenomena in the quantum-Hall analog of the Fabry-Perot interferometer, exploring the roles of the Aharonov-Bohm effect, Coulomb interactions, and fractional statistics on the oscillations of the resistance as one varies the magnetic field B and/or the voltage V_G applied to a side gate. Coulomb interactions couple the interfering edge mode to localized quasiparticle states in the bulk, whose occupation is quantized in integer values. For the integer quantum Hall effect, if the bulk-edge coupling is absent, the resistance exhibits an Aharonov-Bohm (AB) periodicity, where the phase is equal to the number of quanta of magnetic flux enclosed by a specified interferometer area. When bulk-edge coupling is present, the actual area of the interferometer oscillates as function of B and V_G , with a combination of a smooth variation and abrupt jumps due to changes in the number of quasi-particles in the bulk of the interferometer. This modulates the Aharonov-Bohm phase and gives rise to additional periodicities in the resistance. In the limit of strong interactions, the amplitude of the AB oscillations becomes negligible, and one sees only the new “Coulomb-dominated” (CD) periodicity. In the limits where either the AB or the CD periodicities dominate, a color map of resistance will show a series of parallel stripes in the $B - V_G$ plane, but the two cases show different stripe spacings and slopes of opposite signs. At intermediate coupling, one sees a superposition of the two patterns. We discuss dependences of the interference intensities on parameters including the temperature and the backscattering strengths of the individual constrictions. We also discuss how results are modified in a fractional quantized Hall system, and the extent to which the interferometer may demonstrate the fractional statistics of the quasiparticles.

PACS numbers: 73.43.Cd, 73.43.Jn, 85.35.Ds, 73.23.Hk

I. INTRODUCTION

A. Background

In the last few years there has been a surge of interest in electronic interference phenomena in the regime of the quantum Hall effect. This interest, both theoretical¹⁻⁷ and experimental⁸⁻²³, results in large part from the hope of utilizing interference to probe unconventional statistics in various fractional quantum Hall states. Interestingly, interferometer experiments have led to puzzling results even in the integer regime, which have posed a challenge to our theoretical understanding.

Arguably the simplest realization of a quantum Hall interferometer is an analog to the optical Fabry-Perot device. It is constructed of a Hall bar perturbed by two constrictions, each of which introduces an amplitude for inter-edge scattering. (See Figure 1) The backscattering probability of a wave packet that goes through the constrictions is then determined by an interference of trajectories. In the limit of weak inter-edge scattering, two trajectories interfere, corresponding to scattering across each of the two constrictions. As the scattering amplitudes get larger, multiple reflections play a more significant role.

In our analysis, we assume that the two constrictions forming the interferometer are identical to each other, and that there is a single partially-transmitted edge channel penetrating the two constrictions. This partially

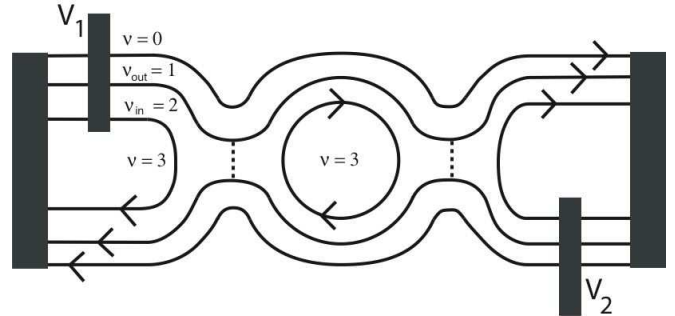


FIG. 1: Fabry-Perot interferometer with $f_T = 1$ totally transmitted edge modes. Filling factor at the center of the constriction is in the range $1 < \nu_c < 2$ and the partially transmitted edge mode separates quantized Hall regions with nominal filling $\nu_{out} = 1$ and $\nu_{in} = 2$. A third edge mode is totally reflected before entering the constrictions, as the bulk filling factor in the center of the interferometer lies in the range $2.5 < \nu_b < 3.5$. Dotted lines in each constriction show the locations of backscattering between the two edges.

transmitted channel separates two quantized Hall states corresponding to rational filling factors $\nu_{in} > \nu_{out}$, with ν_{out} being closer to the sample edge. In addition to the interfering channel, there may be a number of outer edge channels that are fully transmitted through the two constrictions, whose number we denote by $f_T \geq 0$. The situations considered in this paper assume that the states ν_{in}

and ν_{out} are either integer states or integers plus a fraction described in the composite fermion picture, where the partially filled Landau level is less than half full. In particular, this means that all edge states propagate in the same direction. We refer to the cases where ν_{in} is integer or fractional as IQHE and FQHE interferometer, respectively.

For non-interacting electrons, there will be an interference between electrons backscattered at the two constrictions, with a relative phase determined by the Aharonov-Bohm effect. It is periodic in the magnetic flux Φ enclosed by the loop defined by the two interfering trajectories, with a period of one flux quantum Φ_0 (we define the flux quantum as $\Phi_0 = h/|e| > 0$, where $e < 0$ is the electron charge.). For a uniform magnetic field B the flux is $\Phi = BA_I$, with A_I being the area of the interference loop. Experimentally, it is customary to affect this flux through two experimental knobs: B the magnetic field, and V_G , the voltage on a gate that affects the area of the loop. The gate may be positioned above the interference loop or to its side. For fractional quantum Hall states, where electron-electron interaction is essential, the relative phase is made of two contributions, an Aharonov-Bohm phase that is scaled down by the charge of the interfering quasi-particle, and an anyonic phase, accumulated when one quasi-particle encircles another.

Experimentally, several remarkable observations were made^{10,12,13,16,19} when interference was measured in small Fabry-Perot interferometers, e.g. with an interference loop whose area is around $5\mu m^2$. One observation was that when the magnetic field is varied, the backscattering current oscillates as a function of the magnetic field, but the period ΔB of the oscillations was not Φ_0/A_I . Rather, it was given by $\Phi_0/f_T A_I$, which means, in particular, that there was no dependence on B for $f_T = 0$. The period ΔB did not change when ν_c , the filling factor at the center of the constriction was varied in the range between f_T and $f_T + 1$, and the back scattering probability for the partially transmitted edge state varied from strong to weak. Second, when the lines of constant phase in the $B - V_G$ plane were examined^{13,16}, they were found to have positive slope, which is opposite sign relative to what one would naively expect for an Aharonov-Bohm interference effect (Similar lines were observed also in Ref. [20], where a scanning probe was used to probe the spectrum of excitations of a spontaneously formed quantum dot). By contrast, in interferometers that are sufficiently large (e.g., area around $17\mu m^2$), where the center island is covered by a screening top gate, the conventional Aharonov-Bohm pattern was observed, with field period Φ_0/A_I and negative slope for the lines of constant phase. A similar Aharonov-Bohm behavior was also observed in some small interferometers^{17,18}.

Previous works have explained that the periodicities and slopes in the Fabry-Perot interferometer are affected by the Coulomb interactions and the discreteness of electronic charges^{6,13,16}. The regime of parameters where lines of constant phase have positive slope (or zero slope

in the case $f_T = 0$) will be referred to as the Coulomb-Dominated (CD) regime, in contrast with the Aharonov-Bohm (AB) regime.

In this article, we present a general picture of the interplay of the AB and CD regimes in the Fabry-Perot interferometer, and elucidate the way this interplay is determined by the combination of Coulomb interaction and charge discreteness. We limit our analysis of the FQHE to abelian states. We hope to extend our present study to the case of non-abelian states in a future publication.

B. Summary of our results

Before we turn into a detailed discussion, we summarize our results and present a physical way of understanding them. Generally, when electron-electron interactions are taken into account, we find that the area A_I enclosed by the interfering edge state is not a smooth monotonic function of the magnetic field and gate voltage. Rather, we find that A_I has the form

$$A_I = \bar{A}(B, V_G) + \delta A_I, \quad (1)$$

where \bar{A} is a slowly varying function of its arguments, while δA_I has rapid oscillations, on the scale of one flux quantum or on a scale of a change in V_G that adds one electron. (We assume that the area A_I is large enough to enclose many electrons and flux quanta, so that the oscillations occur on a scale where there is only a small fractional change in B or \bar{A} . We shall also assume, unless otherwise stated, that the secular area \bar{A} is only weakly dependent on the magnetic field B , i.e., that $B\partial\bar{A}/\partial B$ is negligible compared to \bar{A} .) The oscillatory dependence of δA_I on the magnetic field and V_G can have striking consequences on the interference pattern, as we shall see below.

Typically, experiments measure the ‘‘diagonal resistance’’ R_D [23], which is essentially the two-terminal Hall resistance of the interferometer region. We find that R_D has an oscillatory part δR , which is a periodic function of B and δV_G . In the limit of weak backscattering it may be written as

$$\delta R = \text{Re} \left(\sum_{m=-\infty}^{\infty} R_m e^{2\pi i(m\phi + \alpha_m \delta V_G)} \right), \quad (2)$$

where

$$\phi \equiv B\bar{A}/\Phi_0, \quad (3)$$

and the coefficients R_m , α_m are real and only slowly varying functions of B , V_G . The voltage V_G affects the phases $e^{2\pi i(m\phi + \alpha_m \delta V_G)}$ in (2) in two ways. First, it affects the flux ϕ through its effect on the area \bar{A} . Second, it affects the density in the bulk of the interferometer, indirectly affecting the interference through interactions of the edge with the bulk. The coefficients α_m quantify the latter effect, which we will analyze further below.

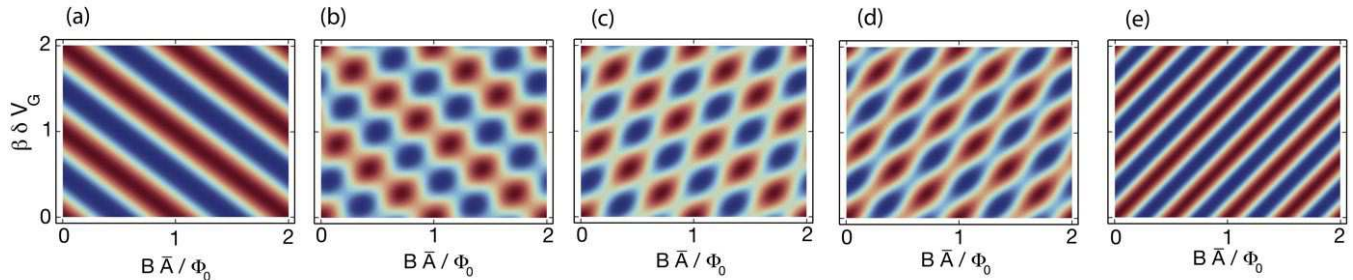


FIG. 2: $\langle \delta R \rangle = \text{Re}(R_1 e^{2\pi i \phi} + R_{-f_T} e^{-2\pi i f_T \phi})$ as a color map in the plane of B and V_G , for $f_T = 2$, with the parameter γ chosen equal to 3.5β . Panels (a), (b), (c), (d), and (e), have, respectively $|R_{-2}/R_1| = 0, 0.5, 1, 2, \text{ and } \infty$, corresponding to the AB, mixed and CD regimes. All Fourier components other than $m = 1$ and $m = -f_T$ are neglected. Alternating red and blue regions represent positive and negative values, respectively, while white signifies a value close to zero.

For non-interacting electrons (the extreme AB limit), the weak backscattering limit has only one non-zero component in Eq. (2). That component is $m = 1$, with $\alpha_1 = 0$. Since the area \bar{A} should be a monotonically increasing function of V_G , we find that for small changes in B and V_G the contours of constant phase are straight lines of negative slope in the $B - V_G$ plane. (When backscattering becomes stronger, multiple reflections lead to more harmonics of m showing up, but still $\alpha_m = 0$, so the slope does not change.) When plotted as a color-scale map in a $B - V_G$ plane, the resistance R_D forms a set of parallel lines, such as the dominant features seen in Fig. [2a].

Electron-electron interactions lead to two important differences between the quantum Hall interferometer and a naive Aharonov-Bohm interference experiment. First, as mentioned above, the area A_I of the interference loop is not rigidly constrained a priori, but can fluctuate slightly. Thus, the area of the interference loop varies with magnetic field and the flux within the loop is generally not a simple linear function of the magnetic field. The position of the edge is related to the charge it encloses, and its variation in our model is a consequence of considerations of energy. Second, we model the region enclosed by the interference loop as one in which there are localized states close to the chemical potential. The number N_L of electrons (in the IQHE regime) or quasi-particles (in the FQHE regime) that are localized in the bulk is an integer, and varies discretely. Due to considerations of energy, an abrupt change of occupation of a localized state as the magnetic field is varied affects also the position of the interfering edge, and hence induces an abrupt change in the flux enclosed by the interference loop.

Thus, as B or V_G vary, the phase accumulated by the interfering particle, θ , evolves in two ways: continuous evolution for as long as N_L does not vary, and abrupt jumps for magnetic fields at which N_L abruptly changes. The continuous change results from the variation of the

magnetic flux in the interference loop, both directly as a consequence of the varying B , and indirectly as a consequence of the variation of the loop's area A_I . The abrupt change results from the effect of a variation of N_L on the area of the interference loop, and, in the FQHE, from the anyonic phase accumulated when fractionally charged quasi-particles encircle one another. Specifically, in the integer case, θ is simply related to the field B and the area A_I by

$$\theta = 2\pi B A_I / \Phi_0, \quad (4)$$

while, for the FQHE states that we consider, we have

$$\theta = 2\pi e_{in}^* \frac{B A_I}{\Phi_0} + N_L \theta_a, \quad (5)$$

where θ_a is the phase accumulated when one elementary quasi-particle of charge of the inner FQHM state ν_{in} encircles another, and e_{in}^* is the charge of the quasiparticle. Here, and in the following, charge is to be measured in units of the (negative) electron charge e .

Within our model, both the rate of continuous evolution of the phase, $d\theta/d\phi$, and the size $2\pi\Delta$ of the phase jump associated with a change of N_L by -1, vary only slowly with B and V_G . The same holds for the magnetic field spacings between consecutive changes in N_L .

In the extreme Coulomb dominated regime, for integer and fractional states alike, we find that a change of N_L is accompanied by a change of the area of the interference loop in such a way that the phase jump $\Delta\theta$ is an unobservable integer multiple of 2π . Coulomb interaction makes the area vary in such a way that the continuous variation of the phase follows $\frac{d\theta}{d\phi} = -2\pi \frac{\nu_{out}}{e_{out}^*}$, where e_{out}^* is the elementary charge of the outer ν_{out} quantized Hall state. Neglecting the unobservable phase jumps, then, $\theta = -2\pi \frac{\nu_{out}}{e_{out}^*} \phi$ for both the IQHE and the FQHE. This limit characterizes interferometers where the capacitive coupling of the bulk and the edge is strong. By contrast, in the extreme Aharonov-Bohm case, where the bulk and

the interfering edge are not coupled, the area of the interference loop does not vary with B at all. Moreover, A_I does not vary when N_L varies. Thus, for integer states $\theta = 2\pi\phi$. The fractional case is more complicated due to the anyonic phase θ_a .

In between these two extremes, θ is not proportional to ϕ , and thus the Fourier transform of $e^{i\theta}$ with respect to ϕ has more than one component. For fractional states this is the case even in the extreme AB limit, due to the anyonic phase θ_a . We find that for all the cases we consider, the components that appear in Eq. (2) satisfy

$$m = -\frac{\nu_{out}}{e_{out}^*} + g\frac{\nu_{in}}{e_{in}^*}, \quad (6)$$

where g is an integer. Note that the ratios ν_{out}/e_{out}^* and ν_{in}/e_{in}^* are always integers, so the allowed values of m are integers as well. Moreover, due to the interaction, α_m is not proportional to m , leading to different slopes of the equal phase lines for the different m components.

The Coulomb dominated limit and the Aharonov-Bohm limit are both defined in terms of the dominant values of g in (6). In the extreme CD limit the only term that appears in the sum (2) is that of $g = 0$ in (6), both for integer and fractional states. In the extreme AB limit of integer states the only term that appears in (2) is the naive Aharonov-Bohm term $m = 1$ (or $g = 1$ in (6)). For fractional states, however, there will be coupling due to the phase jumps associated with the anyonic statistics of the quasi-particles, and one would not find pure AB behavior, (only $g = 1$), even when the Coulomb coupling between N_L and A_I can be neglected. Moreover, for FQHE states with $\nu_{in} > 1$, one finds that there is no value of g that generates $m = 1$ in Eq. (6), so the naive AB period is completely absent in the weak backscattering limit.

In between the extreme Aharonov-Bohm and Coulomb-dominated limits, all integers g appear in the Fourier decomposition of δR , with the relative dominance of the AB and CD components being determined by the value of Δ . We find, under plausible assumptions, that $0 < \Delta < 1$, and that if $0 \leq \Delta < 1/2$ the AB term will dominate, whereas the CD term will dominate if $1/2 < \Delta \leq 1$.

When the sum (2) is dominated by one term, as is the case in the CD limit and the AB limit of the IQHE, the color-scale plot of δR on the $B - V_G$ plane is characterized by a set of parallel lines, as is the case in Figs. [2a] and [2e].

The three figures [2b]-[2d] show the intermediate case, in which several values of m contribute, and α_m is not proportional to m . Then the structure of R_D in the $B - V_G$ plane assumes a form of a two-dimensional lattice, rather than a set of lines, as it would if α_m stayed proportional to m . The periodic structure may be characterized by a unit cell in the $B - V_G$ plane, described by two elementary lattice vectors \mathbf{b} and \mathbf{v} . In the most general case these vectors can have two arbitrary orientations in the plane. However, if the secular area \bar{A} is

only weakly dependent on the magnetic field B , that is if $B\partial\bar{A}/\partial B \ll \bar{A}$, we find that one of the elementary lattice vectors will be parallel to the B axis. Specifically, if V_G is held constant, δR will be unchanged when B is changed by the amount that increases ϕ by one. (We emphasize that this is true even if the interfering particles are fractionally charged.) In our later discussions, rather than employing the direct lattice vectors \mathbf{b} and \mathbf{v} , we shall use a description in terms of their reciprocal lattice vectors.

The restriction of the Fourier harmonics to the values (6) is valid only in the limit of weak backscattering. As the constrictions are further closed and the amplitude for backscattering becomes appreciable, all values of m appear in (2). In the limit where this amplitude is strong, oscillations in the reflection probability turn into transmission resonances. The spacing between these resonances varies with the degree of coupling between the bulk and the edge. Generally, a transmission resonance occurs when the almost closed interfering edge has a degeneracy point, at which it may accommodate an extra electron (for the IQHE) or quasi-particle (for the FQHE) at no extra energy cost. In the Aharonov-Bohm limit, it is the energy of the edge, decoupled from the localized charges it encloses, that should be invariant to adding an extra charge carrier. At the integer quantum Hall regime, that would give rise to one transmission resonance per every flux quantum. In the Coulomb Dominated limit, when the introduction of localized charges affects the energy of the edge through their mutual coupling, there would be ν_{out}/e_{out}^* resonances per quantum of flux, in both the IQHE and the FQHE. Thus, the distinction between the AB and CD limits holds even in the limit of a closed interferometer, where the interfering edge almost becomes a quantum dot.

As should be clear from the discussion above, the form of δR depends crucially on the continuous and abrupt phase variations $d\theta/d\phi$ and $\Delta\theta$. Both of these quantities depend on energy considerations, since the interferometer's area is a property of thermal equilibrium. We model the energy of the interferometer in terms of a capacitor network. The parameters of the model, describing the self capacitance of the interfering edge, the self capacitance of the localized quasi-particles, the mutual capacitance of the two, and the capacitive coupling of the gate to the interferometer, depend on microscopic parameters which we cannot accurately calculate at this point. However, we are able to give some insights into the way in which various parameters should vary with details of the systems, including particularly the perimeter and area of the interference loop.

C. The structure of the paper

The structure of the paper is as follows. In Sec. (II) we deal with the weak backscattering limit. We identify what we believe to be the important degrees of freedom in the interferometer, express the phase θ in terms of these

symbol	short description	section
ν_{in} (ν_{out})	filling factor inside (outside) the interfering edge state	I A
f_T	number of fully transmitted edge states	I A
B	magnetic field	I A
ΔB	magnetic field periodicity	I A
V_G	voltage applied to a gate	I A
A_I	area of the interference loop	I A
\bar{A}	slowly varying part of A_I	I B
δA_I	rapidly oscillating part of A_I	I B
R_D	diagonal resistance	I B
δR	oscillatory part of R_D	I B
ϕ	magnetic flux within the area \bar{A}	I B
α_m	quantifies the effect of V_G on the bulk of the interferometer loop	I B
N_L	number of electrons or quasi-particles localized in the bulk of the interferometer	I B
θ	the interference phase	I B
e_{in}^* (e_{out}^*)	the charge of a quasi-particle in the ν_{in} (ν_{out}) state	I B
$2\pi\Delta$	jump in phase θ when N_L varies by -1	I B
θ_a	anyon phase	I B
r_1, r_2	reflection amplitudes at constrictions 1,2	II
N_j^e, N_j^h	integer number of localized electrons and holes in the j 'th Landau level	II
K_I, K_{IL}, K_L	coupling constants in the energy functional describing the interferometer	II A
\bar{q}	effective bulk background charge	II A
β	quantifies the effect of V_G on the area of the interferometer	II A
γ	quantifies the effect of V_G on the bulk background charge	II A
$\Delta\nu$	$\nu_{in} - \nu_{out}$	II B
C_I, C_L, C_{IL}	re-parametrization of K_I, K_L, K_{IL} by effective capacitances	II C
μ_I, μ_L	electro-chemical potentials of the I and L regions	II C
w, L	width and length of the region of non-uniform density near the loop's edge	II C
Z	partition function	III B
\vec{G}_{gh}	reciprocal lattice vectors of the 2D description of $\delta R(B, V_G)$	III E
λ	describes the variation of \bar{A} with B	III E
η	describes the variation of \bar{q} with B	III E
P_R	reflection probability for the interfering edge state	IV
χ_{\pm}	interferometer scattering phase shifts	IV
$\rho(\epsilon)$	density of states	IV
$\Delta\phi$	flux spacing between resonances	V
N_o	total number of electrons in the highest Landau level enclosed by the interfering edge channels	V

TABLE I: List of symbols, their brief description, and the section where they are defined

degrees of freedom and introduce an energy functional in terms of these degrees of freedom. In Sec. (III) we calculate the thermal average of $e^{i\theta}$, which is the factor that determines the interference contribution to R_D in the weak backscattering limit, and distinguish between the Aharonov-Bohm and Coulomb-Dominated limits. In Sec (IV) we extend the discussion to the regime of intermediate backscattering, and in Sec. (V) to the regime of strong backscattering. In Sec. (VI) we exemplify the way in which the energy parameters for the interfering edge and the localized states can be influenced by coupling to edge states that are fully transmitted, by solving in detail two simple models. In Sec. (VII) we compare our findings to earlier experimental and theoretical works. Finally, we summarize our results in Sec. (VIII).

For the convenience of the reader, we include a table with a list of the main symbols used in the paper, their brief description, and a pointer to the Section in which they are defined.

II. THE PHYSICAL MODEL - WEAK BACKSCATTERING CASE

In this section we introduce the physical model on which we base our analysis of the weak backscattering limit. We start with the IQHE interferometers, and then generalize to the FQHE ones.

In the weak backscattering limit there should be an oscillatory part of the backscattered resistance given by

$$\delta R \propto \text{Re}[r_1 r_2^* \langle e^{i\theta} \rangle] \quad (7)$$

where r_1, r_2 are the reflection amplitudes at the two constrictions, and the angular brackets represent an average over thermal fluctuations. We focus here on measurements in the limit of small source-drain bias, so we may consider all leads to be at the same electrochemical potential μ . We assume the change in B and V_G to be small enough that we may neglect any changes in r_1 and r_2 , and associate oscillations in the resistance with oscillations in the phase factor $\langle e^{i\theta} \rangle$.

Our analysis of the phase factor $e^{i\theta}$ is based on the following picture of the edge of a quantum Hall fluid in the integer regime. We expect that any Landau level j which is more than half filled in the bulk of the system will have a single chiral edge state that circulates along the edge of the system. To the extent that the electron density varies smoothly near the edge of the sample, on the scale of the magnetic length, we expect that the spatial location of the edge state will be close to the point where the Landau level is half-full. In typical situations, we will not find that electronic states in the Landau level are entirely empty at positions outside the edge state or entirely full inside the edge state. Rather, the Landau level will have a certain number of electrons N_j^e in localized states outside the edge state, and a certain number N_j^h of unoccupied localized states (holes) inside the edge state. The quantities N_j^h and N_j^e are constrained to be

integers, as they represent the occupations of localized states.

In our analysis we will neglect the electrons and holes localized between edge states, and consider only those that are localized in the bulk of the sample, where the filling factor is ν_{in} . This neglect is justified below, towards the end of this section. We shall also assume that the electrons that are localized in the ν_{in} bulk region are weakly conducting and compressible over long time scales, so that we can view them as forming a metallic region of a uniform electro-chemical potential, whose number of electrons is quantized to an integer N_L .²⁴ Experimental support for this picture was found in [20]. Both of these assumptions are further elaborated on towards the end of this section.

Within this model, then, the interferometer has a single discrete degree of freedom, N_L , and several continuous degrees of freedom A_j , describing the area (relative to a reference area) occupied by each of the edges that are coupled to the leads (the subscript numbers the edge state). As is always the case in the quantum Hall effect, charge density on the edge translates to an area enclosed by the Landau level. The phase θ is directly related to the area A_I enclosed by the interfering edge state, as delimited by the points in the constrictions where there is tunneling between the partially transmitted edge states. (The subscript I stands for ‘‘interfering’’). Specifically, the relation is given in Eq. (4), above. Alternatively, we can consider θ as a measurable quantity (mod 2π), and use (4), to form a precise definition of A_I .

A. Macroscopic energy function

We will now formulate the way by which we will calculate (7) and its dependence on B and V_G . Since the phase θ depends only on what happens in the ν_{in} bulk region, we find it useful to define an energy functional $E(N_L, A_I)$ as the total energy of the system when N_L and A_I are specified, and the energy is minimized with respect to all other variables, including the fluctuating areas A_j of any fully transmitted edge states. (The electrochemical potential μ of the leads is here taken to be zero.).

Let us consider small variations of B about a given initial value B_0 , at a fixed value of the gate voltage V_G . For small variations in N_L, A_I , we may then expand the energy $E(N_L, A_I)$ to quadratic order, and write

$$E = \frac{K_I}{2} (\delta n_I)^2 + \frac{K_L}{2} (\delta n_L)^2 + K_{IL} \delta n_I \delta n_L, \quad (8)$$

where δn_L is the deviation of the number of localized electrons from the value that would minimize the energy if there were no integer constraint on N_L , and δn_I is the deviation of the charge on the interfering edge, in units of the electron charge, from the charge that would then

minimize the energy. More precisely,

$$\delta n_L = N_L + \nu_{in}\phi - \bar{q} \quad (9)$$

where \bar{q} is the effective positive background charge, in units of $|e|$, resulting from ionized impurities in the donor layer and additional charges on the surfaces and on metallic gates, as well as any fixed charges in localized states outside the interference loop. We assume that \bar{q} depends monotonically on the gate voltage. Furthermore, for weak backscattering,

$$\delta n_I = B(A_I - \bar{A})/\Phi_0 = n_I - \phi, \quad (10)$$

where n_I is the charge enclosed by the interfering edge state, ignoring the charges of the localized electrons and holes.

When the gate voltage V_G is varied with B remaining fixed, the background charge \bar{q} and the area \bar{A} will vary. Their variation depends on the coupling of the gate to the interferometer, and we characterize it by two parameters:

$$\beta = (B/\Phi_0)d\bar{A}/dV_G, \quad \gamma = d\bar{q}/dV_G. \quad (11)$$

The parameter β describes the extent to which a variation of the gate voltage affects the area of the interferometer A_I (and indirectly ϕ), while γ describes the way the gate affects the background charge in the bulk of the interferometer (and indirectly N_L).

Note that the energy function (8) leads to an interference phase that is unchanged when ϕ varies by one. This change in ϕ can be completely compensated in the energy function by changing N_L by the integer amount $-\nu_{in}$, while n_I changes by one. The fixed value of δn_I means that the area A_I has not changed, but the phase θ has changed by 2π . Such a phase change has no effect on the value of $e^{i\theta}$.

B. Fractional quantized Hall states

Our considerations for the integer case can be easily extended to fractional quantized Hall states of the form

$$\nu_{in} = I + \frac{p}{2ps+1}, \quad \nu_{out} = I + \frac{p-1}{2s(p-1)+1}, \quad (12)$$

where p and s are positive integers, and $I \geq 0$ is an integer. These are filling fractions in the range $I \leq \nu < I + 1/2$, and we assume that they are correctly described by the standard composite fermion picture. Moreover, we assume that the backscattered excitation is the elementary quasiparticle of the state ν_{in} , with charge $e_{in}^* = 1/(2sp+1)$. We again use a quadratic energy function of the form (8), but now we have to modify (9) and (10) and use (5) instead of (4) to describe the relations between $\delta n_I, A_I, N_L$ and θ .

Specifically, the phase θ accumulated by an interfering quasi-particle is

$$\frac{\theta}{2\pi} = e_{in}^* B A_I / \Phi_0 - 2N_L s e_{in}^*. \quad (13)$$

The first term is the Aharonov-Bohm phase, scaled down by the charge of the interfering quasi-particle, and the second term is the anyonic phase accumulated when one composite fermion goes around another.^{25–27} The statistical phase θ_a , which appeared in Eq. (5), is thus given by $\theta_a = -4\pi s e_{in}^*$.

An increase of the magnetic flux by one flux quantum introduces, on average, ν_{in}/e_{in}^* quasi-particles, hence modifying (9) to be

$$\delta n_L = e_{in}^* N_L + \phi \nu_{in} - \bar{q} \quad (14)$$

Here N_L is the net number of quasiparticles minus quasi-holes, of charge e_{in}^* , inside the interfering edge state.

The relation between the area enclosed by the interfering edge and the charge contained in the corresponding composite fermion Landau level – the modified version of (10) – is,

$$\delta n_I = \Delta \nu B(A_I - \bar{A})/\Phi_0, \quad (15)$$

where $\Delta \nu \equiv \nu_{in} - \nu_{out}$. The normalizations of δn_I and δn_L have been chosen so that they are measured in units of the electron charge.

As before, in the limit of weak back scattering, the resistance oscillation will be proportional to $\text{Re} \langle e^{i\theta} \rangle$. Note that formulas for the fractional case reduce to those of the integer case if one sets $s = 0$.

C. Comments on the energy function

The previous subsection has defined the model we will use for analyzing the interference term (7) and its dependence on B and V_G . Before carrying out this calculation, we pause to make some comments on the model.

1. An alternative parametrization of the energy function

The macroscopic energy function E may be alternatively described by an equivalent capacitor network. If we introduce electrochemical potentials $\mu_I = \partial E/\partial(\delta n_I)$, and $\mu_L = \partial E/\partial(\delta n_L)$, then the quadratic part of E may be rewritten as

$$e^2 E = \frac{C_I}{2} \mu_I^2 + \frac{C_L}{2} \mu_L^2 + \frac{C_{IL}}{2} (\mu_I - \mu_L)^2, \quad (16)$$

where

$$K_I = e^2 \frac{C_L + C_{IL}}{D}, \quad K_L = e^2 \frac{C_I + C_{IL}}{D}, \quad K_{IL} = e^2 \frac{C_{IL}}{D},$$

$$D = (C_L + C_{IL})(C_I + C_{IL}) - C_{IL}^2. \quad (17)$$

The coefficients C_L and C_I may be interpreted as effective capacitances to ground for the respective conductors, while C_{IL} plays the role of a cross-capacitance. The effective capacitances result from a combination of classical electrostatics and quantum mechanical energies.

An advantage of rewriting the energy in this form is that it may be easier to understand the dependencies of the capacitance coefficients on the parameters of the system. For example, we would expect the coefficients C_I and C_{IL} to be proportional to the perimeter L of the interferometer, if the structure of the edge is held fixed. The capacitance C_L should be proportional to the area \bar{A} of the island, if the center region is covered by a top gate with a fixed set-back distance. On the other hand, we would expect C_L to vary as $L \log L$, if there is no top gate and the nearest conductors are gates along the edges of the sample.

In the situation where the edge state is connected to leads in equilibrium at zero voltage, the equilibrium value of μ_I will be zero. Then the ground state energy will be given by $E = (C_L + C_{IL})\mu_L^2/2e^2$, and we have $e^2 \delta n_L = \mu_L(C_L + C_{IL})$ and $e^2 \delta n_I = -\mu_L C_{IL}$.

2. Further justification for the model

The major simplification involved in our model is the reduction of the number of degrees of freedom in the problem. In principle, the interferometer has edge states that form one-dimensional compressible stripes and a set of localized states between these stripes that may be either empty or full. Our model reduces the problem to two degrees of freedom, A_I and N_L .

We use one number, N_L , to describe the number of localized states in the bulk of the interferometer based on the assumption that electrons or holes in a localized state are localized in a one-body approximation, but are not completely immobile. At any finite temperature, they have a non-zero conductivity due to processes such as multi-particle hopping, and we assume that they can readjust their relative positions continuously. Thus, on a laboratory time scale, the interior of the island should behave like a metal: the N_L charges arrange themselves to give a constant electrochemical potential in equilibrium, within each class of localized states.²⁴ As a result of the integer constraints on the total occupation numbers, however, there can be small differences between the electrochemical potentials of the localized states and that of the adjacent edge states or leads.

We neglect the degrees of freedom associated with localized states between edge states. We assume again that the width w of the region of non-uniform electron density near the edge of the sample is small compared to the overall radius to the island. The area available for localized electrons or holes in the Landau level that is partially filled in the center of the interferometer should be approximately \bar{A} , while the areas available for localized electrons or holes in any other Landau levels should be of order Lw , which is much smaller. Then the number of localized electrons or holes in any of these regions will be relatively small, and the energy cost of adding or subtracting a particle from one of them should be relatively high. Thus we may generally neglect fluctuations

in these quantities at reasonably low temperatures. The fluctuations in N_L that do occur will arise normally from changes in the occupation of the innermost partially full Landau level.

If the magnetic field B or the gate voltage V_G is varied by a sufficiently large amount, we do expect to encounter discontinuous changes in the occupations of localized states other than those N_L of the inner-most partially full Landau level. These jumps should lead to jumps in the phase θ , which would appear as ‘‘glitches’’ in the interference pattern. The analysis of periodicities given above apply, strictly speaking, only in the intervals between glitches. The frequency of occurrence of glitches should roughly correspond to the addition of one electron or one flux quantum in area Lw , which would be rarer by a factor of Lw/\bar{A} than the oscillation frequencies we are interested in. Also, in many cases, the coupling between the interfering edge state θ and a particular occupation number N_j^h or N_j^e may be sufficiently small that any glitches associated with changes in that occupation number would be unobservable.

Finally, in replacing the full energy function by the macroscopic function E , we have minimized the energy with respect to all continuous variables n_j other than that of the partially transmitted edge state, i.e., we have ignored the effects of thermal fluctuations in these variables. This neglect is justified for the continuous variables, because they enter the energy in a quadratic form, so their thermal fluctuations add only a constant to the energy.

III. AHARONOV-BOHM AND COULOMB-DOMINATED REGIMES IN THE WEAK BACKSCATTERING LIMIT

We now have Eq. (7) for the resistance in the weak backscattering limit in terms of the interference phase θ . We also have Eqs. (4,5, 13) for θ in terms of the degrees of freedom A_I, N_L , and the energy function (8) for the energy and its dependence on B and V_G . In this section we make use of these expressions to calculate several thermal averages. First, we calculate the abrupt phase jump $2\pi\Delta$ that occurs when the number of localized electrons (or quasi-particles) varies by -1 . Then, we calculate the magnetic field and gate voltage dependencies of $\langle e^{i\theta} \rangle$ at high temperatures, and show that in that limit the interferometer shows either AB or CD behavior, depending on the value of Δ . Finally, we turn to the case where AB and CD behaviors mix together, and develop the tools needed to analyze this case, at low temperatures as well as high.

A. Continuous and abrupt phase evolution

As the energy function is quadratic with respect to the continuous variable A_I , the average A_I is the one

that minimizes the energy function. For a fixed number N_L of localized charges, we obtain

$$\frac{\theta}{2\pi} = e_{in}^* \phi - 2s e_{in}^* N_L - \frac{K_{IL}}{K_I} \frac{1}{e_{out}^*} [e_{in}^* N_L + \nu_{in} \phi - \bar{q}] \quad (18)$$

The abrupt phase jumps $2\pi\Delta$ associated with a change of N_L by -1 can be read out from (18). For an IQHE interferometer we find

$$\Delta = \frac{K_{IL}}{K_I} = \frac{C_{IL}}{C_L + C_{IL}} \quad (19)$$

When there is no bulk-edge coupling $K_{IL} = 0$ the interference phase is unaffected by N_L . When the bulk-edge coupling is strong, the jumps are unobservable, since $\Delta = 1$.

For an FQHE interferometer, we have

$$\Delta = \frac{K_{IL}}{K_I} + 2e_{in}^* s \left(1 - \frac{K_{IL}}{K_I} \right) \quad (20)$$

Now, if $K_{IL} = 0$, then $2\pi\Delta$ is the phase jump associated with the fractional statistics of the quasi-particles. When the bulk and the edge are coupled, the phase jumps reflect both the change of the area A_I caused by the introduction of quasi-particles and the fractional statistics. In the limit of strong coupling, where $K_{IL} = K_I$, the phase jump becomes unobservable, just as in the integer case. Now, if there is a change of -1 in N_L , corresponding to the introduction of a quasi-hole in the bulk, the area A_I will increase by $(e_{in}^*/\Delta\nu)(\Phi_0/B)$. This is the area necessary to accommodate the charge of the quasi-hole, and is also the area necessary for the accumulated phase to grow by 2π .

B. Magnetic field dependence

Next, if the parameters entering (8) are known, we may calculate the thermal expectation value

$$\langle e^{i\theta} \rangle = Z^{-1} \sum_{N_L} \int_{-\infty}^{\infty} dA_I e^{-E/T} e^{i\theta}, \quad (21)$$

with the partition function Z given by

$$Z = \sum_{N_L} \int_{-\infty}^{\infty} dA_I e^{-E/T}. \quad (22)$$

Since E is a quadratic function of its variables, the integration over A_I is trivial. The sum over the discrete variable N_L can be handled by using the Poisson summation formula and taking the Fourier transform. Thus we may write

$$\sum_{N_L=-\infty}^{\infty} = \int_{-\infty}^{\infty} dN_L \sum_{g=-\infty}^{\infty} e^{-2\pi i N_L (g-1)} \quad (23)$$

Using this formula, one may perform the integrations over N_L in the numerator and denominator of (21). The formulas simplify at high temperatures, where the partition function Z becomes independent of ϕ , and we may concentrate on the numerator of (21). We then find that the expectation value can be written in the form

$$\langle e^{i\theta} \rangle = \sum_{g=-\infty}^{\infty} D_m e^{2\pi i m \phi}, \quad (24)$$

where $m(g) = -\frac{\nu_{out}}{e_{out}^*} + g \frac{\nu_{in}^*}{e_{in}^*}$, as in Eq. (6).

The coefficients D_m may be written as

$$D_m = (-1)^{g+1} |D_m| \exp \left[2\pi i \bar{q} \left(\frac{e_{in}^* - m}{\nu_{in}} \right) \right], \quad (25)$$

with

$$|D_m| = e^{-2\pi^2 T/E_m} \quad (26)$$

and

$$\frac{1}{E_m} = \frac{1}{(e_{out}^*)^2 K_I} + \frac{(g-1+\Delta)^2 K_I}{(e_{in}^*)^2 (K_I K_L - K_{IL}^2)} \quad (27)$$

Remarkably, Eq. (27) identifies the most dominant Fourier component of the resistance in the high temperature limit, and displays its relation to Δ : in the integer case and for fractions where $m = 1$ is allowed (i.e., for fractions in with $\nu_{in} < 1/2$), if $-1/2 < \Delta < 1/2$ the interference is dominated by the AB component, with $g = 1, m = 1$. In contrast, if $1/2 < \Delta < 3/2$ it is dominated by the CD component, with $g = 0, m = 1 - (\nu_{in}/e_{in}^*)$.

We note that the plausible assumption of a positive cross capacitance $C_{IL} > 0$ leads to the restriction $0 < \Delta < 1$. We will then find $\Delta < 1/2$ if and only if $C_{IL} < C_L$. We also remark that the energy E_m for the CD term is related to the capacitances by $E_m = (e_{in}^*)^2 / (C_L + C_I)$. The denominator here may be thought of as an effective capacitance resulting from the electrostatic and quantum capacitances of the combined system of the localized charges and the interfering edge state, if the edge state is disconnected from the leads.

C. Gate voltage dependence

A variation of the gate voltage V_G varies the phases of the Fourier components of $\langle e^{i\theta} \rangle$ through its effect on \bar{q} and ϕ in the phases in Eqs. (24) and (25). There are two origins to this dependence - the effect of the gate voltage on the area of the interference loop \bar{A} and its effect on the charge density in the bulk, and through it, on N_L . These two dependencies are described by the parameters β, γ of (11).

For small variations δV_G and δB , we see that $D_m e^{2\pi i m \phi}$ varies proportional to

$$\exp \left(2\pi i \left[\delta V_G (\alpha_m + \beta m) + m \delta B \frac{\bar{A}}{\Phi_0} \right] \right), \quad (28)$$

where the term proportional to β originates from the area change induced by the gate, and the term proportional to

$$\alpha_m = \gamma (e_{in}^* - m) / \nu_{in}. \quad (29)$$

originates from the effect of the gate on the bulk background charge.

For the integer case, we see that lines of constant slope in the AB regime will have $dV_G/dB = -\bar{A}/\Phi_0\beta$, while in the CD regime, the lines of constant slope will have $dV_G/dB = f_T \bar{A}/\Phi_0(\gamma - f_T\beta)$.

We expect that applying positive voltage to a side gate should tend to increase the area \bar{A} , so that the coefficient β should be positive. To estimate γ , let us first consider a model in which there is a constant electron density in the interior of the interferometer, except for a thin region around the edge, and let us imagine that the effect of δV_G is to alter the location of the edge, without changing its density profile, and without changing the electron density away from the edge. In this case we would find $\gamma = \bar{\nu}\beta$, where $\bar{\nu} \geq (f_T + 1/2)$ is the filling factor in the interior. In reality, we would expect that positive δV_G will increase the average density inside, so that γ should be even larger. Thus we expect that the slope of the constant phase lines will be negative for the AB stripes but positive for the CD stripes.

D. Low temperatures

Although at high temperatures we need only consider one Fourier component, at lower temperatures, particularly if Δ is close to $1/2$, the $g = 0$ and $g = 1$ components may both be important. Then a color-scale map of the interference signal versus B and V_G will show lines of both slopes, with a resulting pattern of a checker-board type, as seen in Fig 2. Even if both slopes are present, however, the eye will tend to pick out only the stronger component, if there is a big difference in the amplitudes, as in panels 2b and 2d.

At still lower temperatures, higher harmonics with $g > 2$ and $g < 0$ will also appear. In general one must take into account that Z in the denominator of (21) depends on ϕ . Let us expand Z as

$$Z = \sum_{g=-\infty}^{\infty} z_g e^{2\pi i g (\nu_{in} \phi - \bar{q}) / e_{in}^*}. \quad (30)$$

(The coefficients z_g fall off exponentially with increasing temperature, except for z_0 , which is simply proportional to T .) The Fourier components of $\langle e^{i\theta} \rangle$ will then be a convolution of the Fourier components of Z^{-1} with the Fourier coefficients obtained from the numerator of (21), which are given by (25) and (26). We see that this does not introduce any new Fourier components into the function, but it can affect the relative weights of the different harmonics.

In the limit of low temperatures, the phase θ becomes a saw-tooth function of ϕ , for fixed V_G , and we can simply evaluate the Fourier coefficients of $e^{i\theta}$. Up to a constant phase factor, we find that for the allowed values of m , the coefficients D_m may still be written in the form (25), but now

$$|D_m| = \frac{\sin(\pi\Delta)}{\pi(\Delta + g - 1)} \quad (31)$$

We see that the CD component ($g = 0$) will be largest if $1/2 < \Delta \leq 1$, and the component ($g = 1$) will be largest if $0 \leq \Delta < 1/2$, at $T=0$ as well as at high temperatures.

In our discussions of the temperature-dependence of the interference signal, we have taken into account only classical fluctuations, ignoring quantum fluctuations, which can be important on energy scales larger than $k_B T$. In the FQHE case, quantum fluctuations lead to a renormalization of the tunneling amplitudes, which will typically cause the individual reflection amplitudes r_1, r_2 to decrease with increasing temperature, as a power of $1/T$, in the weak backscattering regime.²⁸ At high temperatures, this decrease should be less important than the exponential decrease of the interference signal arising from classical fluctuations, predicted by Eq. (26), but the power-law dependence should be taken into account at lower temperatures. If one defines a normalized interference signal by dividing the interference term by the total backscattered intensity, $\propto (|r_1|^2 + |r_2|^2)$, then the low temperature power-law dependence should be cancelled.¹ Quantum fluctuations do not lead to a power law dependence of the normalized interference signal on length of the interferometer, in the limit of vanishing temperature and vanishing source-drain voltage.¹

E. Two-dimensional description

For a proper analysis of the regime where the CD and AB lines co-exist, we need to introduce a two-dimensional Fourier transform of δR with respect to B and V_G , rather than the Fourier transform with respect to ϕ at fixed V_G , which we have employed so far. One finds that the periodic pattern can be expanded in terms of a set of “reciprocal lattice vectors” $\vec{G}_{gh} \equiv (G_{gh}^{(b)}, G_{gh}^{(v)})$, where g and h are integers, with

$$\vec{G}_{gh} = g\vec{G}_{10} + h\vec{G}_{01} \quad (32)$$

$$\vec{G}_{10} = 2\pi \left(\frac{\nu_{in} \bar{A}}{e_{in}^* \Phi_0}, \frac{\beta\nu_{in} - \gamma}{e_{in}^*} \right) \quad (33)$$

$$\vec{G}_{01} = 2\pi \left(-\frac{\nu_{out} \bar{A}}{e_{out}^* \Phi_0}, \frac{\gamma - \beta\nu_{out}}{e_{out}^*} \right) \quad (34)$$

and

$$\delta R(B, V_G) = \sum_{gh} R_{gh} e^{i(G_{gh}^{(b)} \delta B + G_{gh}^{(v)} \delta V_G)}. \quad (35)$$

The reality of δR requires that $R_{gh} = R_{-g, -h}^*$.

The set of reciprocal lattice vectors may be derived by first removing the restriction that N_L is an integer. Regardless of the values of K_I, K_L, K_{IL} , the energy can then be minimized by choosing A_I and N_L so that $\delta n_I = \delta n_L = 0$. using (15) and (14). If we then calculate changes in θ using (13), we find that $\delta\theta = G_{11}^{(b)} \delta B + G_{11}^{(v)} \delta V_G$, while $\delta N_L = -(G_{10}^{(b)} \delta B + G_{10}^{(v)} \delta V_G)/2\pi$, with \vec{G}_{gh} defined as in (32) - (34). Here, we have used the relations $\Delta\nu = e_{in}^* e_{out}^*$ and $2s = (e_{out}^* - e_{in}^*)/\Delta\nu$.

In the limit of weak back scattering, the only reciprocal lattice vectors with non-zero amplitudes have $h = \pm 1$. For $h = 1$, the coefficients R_{gh} may be related to the coefficients D_m defined previously, with $R_{g,1} \propto r_1 r_2 D_m$, where m is related to g by Eq. (6) and r_1, r_2 are the bare reflection amplitudes at the two constrictions. For $h = -1$, the coefficients are the complex conjugates of $R_{-g,1}$.

When one goes beyond weak backscattering, as discussed below, one finds harmonics at reciprocal lattice vectors which are arbitrary sums of the ones present in the weak back scattering limit. Thus, one may obtain contributions at all integer values of h , including $h = 0$.

Using the two-dimensional description, we may readily extend our analysis to the situation where one cannot neglect the dependence of the secular area \bar{A} on the magnetic field B . In this case, we should also take into account the change in the “background charge” \bar{q} resulting from the change in \bar{A} . We define two dimensionless parameters,

$$\lambda = -\frac{B}{\bar{A}} \frac{\partial \bar{A}}{\partial B}, \quad \eta = -\frac{\Phi_0}{\bar{A}} \frac{\partial \bar{q}}{\partial B}. \quad (36)$$

Then the formulas for the fundamental reciprocal lattice vectors should be replaced by

$$\frac{\vec{G}_{10}}{2\pi} = \left[\left(\frac{\nu_{in}(1-\lambda) + \eta}{e_{in}^*} \right) \frac{\bar{A}}{\Phi_0}, \frac{\beta\nu_{in} - \gamma}{e_{in}^*} \right] \quad (37)$$

$$\frac{\vec{G}_{01}}{2\pi} = \left[-\left(\frac{\nu_{out}(1-\lambda) + \eta}{e_{out}^*} \right) \frac{\bar{A}}{\Phi_0}, \frac{\gamma - \beta\nu_{out}}{e_{out}^*} \right] \quad (38)$$

If the field B is varied while the gate voltage V_G is held fixed, the field periods associated with the AB term ($g, h) = (1, 1)$ and the CD term ($g, h) = (0, 1)$ are given, respectively, by

$$\bar{A}(\Delta B)_{AB} = \frac{\Phi_0}{(1-\lambda) \left(\frac{\nu_{in}}{e_{in}^*} - \frac{\nu_{out}}{e_{out}^*} \right) + \eta \left(\frac{1}{e_{in}^*} - \frac{1}{e_{out}^*} \right)}, \quad (39)$$

$$\bar{A}(\Delta B)_{CD} = -\frac{e_{out}^* \Phi_0}{\eta + \nu_{out}(1-\lambda)}. \quad (40)$$

If $\eta \neq 0$, the two periods will generally be incommensurate. Then when the magnetic field is varied at constant gate voltage, the resistance will not be a periodic function of B , but rather quasi-periodic. To obtain a periodic

variation, one must vary B and V_G simultaneously, along a line of appropriate slope.

As a simple example, let us assume that $\bar{A}(B, V_G)$ is determined by a contour in the zero-field electron density $n(\vec{r})$ where $n\Phi_0/B = (\nu_{in} + \nu_{out})/2$, and let us assume that \bar{q} is equal to the integral of this density inside the area \bar{A} . Then we find

$$\eta = \frac{\lambda(\nu_{in} + \nu_{out})}{2}, \quad (41)$$

$$\lambda = \frac{1}{\bar{A}} \oint \frac{n(\vec{r})dr}{|\nabla n|}, \quad (42)$$

where the integral is around the perimeter of the area \bar{A} . We see that η and λ will vanish in the limit where the length scale for density variations at the edge is small compared to the radius of the island, (assuming that the density in the bulk is not too close to density at the interfering edge state).

IV. INTERMEDIATE BACKSCATTERING

If one goes beyond the lowest order in the backscattering amplitudes r_1 and r_2 , the above analysis must be modified in several respects. In this Section we confine ourselves to the IQHE case; we come back to the FQHE in the next Section, for the regime of strong back-scattering.

The most obvious change from the weak backscattering limit is that the interference contribution to the resistance R_D is no longer simply proportional to $\text{Re}[r_1 r_2^* e^{i\theta}]$. To be specific, let us consider the case of symmetric constrictions, so that $r_1 = r_2$. We may write $R_D^{-1} = (f_T + 1 - P_R)(e^2/h)$, where $0 < P_R < 1$ is the probability that an incident electron in the partially transmitted edge state will be reflected by the interferometer region. If we continue to define θ as the phase accumulation around the interferometer loop for an electron at the Fermi energy, then the full expression for P_R is

$$P_R = 2|r_1|^2 \frac{1 + \cos \theta}{1 + |r_1|^4 + 2|r_1|^2 \cos \theta} \quad (43)$$

If we expand this in powers of r_1 , we find terms of order $|r_1|^4$ multiplying $\cos^2 \theta$, etc., which we may understand as contributions from electrons that undergo multiple reflections and therefore traverse the circuit more than once. Such terms will add additional harmonics of $e^{2\pi i \phi}$ to the reflection coefficient, and in principle all harmonics will be present. However, the underlying period will not be affected. Moreover, at least at high temperatures, the higher harmonics should fall off faster than the principal AB component ($\propto e^{2\pi i \phi}$) or the principal CD component ($\propto e^{-2\pi i f_T \phi}$) and should not be very noticeable.

In the presence of a significant reflection probability, one should also take into account the fact that in this case the number of electrons enclosed by the partially transmitted edge state is no longer precisely equal to $\theta/2\pi$.

This follows from the the Friedel sum rule, which states that $\rho(\epsilon)$, the density of states for the Landau level inside the interferometer at energy ϵ may be written as

$$\rho(\epsilon) = \frac{1}{\pi} \frac{\partial(\eta_+ + \eta_-)}{\partial \epsilon}, \quad (44)$$

where η_{\pm} are the phase shifts, derived from the eigenvalues $e^{2i\eta_{\pm}}$ of the 2×2 S -matrix for transmission through the interferometer. Explicitly, the eigenvalues are given by

$$e^{2i\eta_{\pm}} = \frac{(1 - |r_1|^2)e^{i\theta} \pm i|r_1|(e^{2i\theta} + 1)}{1 + |r_1|^2 e^{2i\theta}}, \quad (45)$$

and the phase shifts are required to be continuous functions of the energy ϵ . For $|r_1|^2 \neq 0$, this gives an oscillatory contribution to the phase shifts, and an oscillatory contribution to the density of states. Since the electron number n_I is the integral of $\rho(\epsilon)$ up to the Fermi energy, it will also acquire an oscillatory part. Specifically we may write

$$n_I = \pi^{-1}(\eta_+ + \eta_-) + \text{const} = (2\pi)^{-1}\theta + f(\theta), \quad (46)$$

where the phase shifts are evaluated at the Fermi energy, and $f(\theta)$ is periodic, with period 2π .

The oscillatory contribution to n_I will also be manifest when one varies the magnetic field, the gate voltage, or the electrochemical potential μ . For an interacting system, where the number of electrons n_I associated with the interfering edge state is coupled to other variables, such as N_L , or even to continuous variables such as the number of electrons in fully transmitted edge states, an oscillatory component of n_I will lead to an additional oscillatory component to the energy E , which should be taken into account when evaluating the thermal average of P_R . Again, we see that these effects can lead to additional oscillatory contributions at harmonics of the basic periods, giving rise to non-zero amplitudes at arbitrary reciprocal lattice vectors \vec{G}_{gh} , but they should not change the fundamental frequencies \vec{G}_{10} and \vec{G}_{01} .

We can treat the case of intermediate (or strong) back scattering within our general model if we make a few modifications of the definitions. We continue to use the energy formula (8), with the definitions (4) and (9) for θ and δn_L . We continue to define $\delta n_I \equiv n_I - \phi$, as in (10) but we can no longer equate this to $B(A_I - \bar{A})/\Phi_0$. Instead, we must compute n_I using (46). Finally, we must calculate $\langle P_R \rangle$ by averaging (43) with the weight $e^{-E/T}$, integrating over A_I and summing over N_L .

V. STRONG BACKSCATTERING

It is interesting to explore the behavior of the interferometer at low temperatures in the limit of strong backscattering, where the amplitude r_1 is close to unity. For the case $r_1 = r_2$, when θ is an odd integer multiple

of π a resonant tunneling occurs, and $P_R = 0$. Then, for non-interacting electrons, at large r_1 , we would find that the reflection probability P_R is close to unity most of the time, but there would be a series of values of the magnetic field, or of the gate voltage, where in a narrow interval, P_R drops to zero. The actual vanishing of P_R is special to the case where $r_1 = r_2$, but even for an asymmetric case, one would find reductions in P_R in the vicinity of the points where θ is an odd multiple of π .

We now analyze the effect of interactions between electrons on these transmission resonances, and in particular on the flux spacing $\Delta\phi$ between transmission resonances. Interestingly, we find that this spacing is different for interferometers in the AB and CD regimes.

In the limit of strong backscattering the charge enclosed in the ν_{in} area is almost quantized in units of e_{out}^* . The condition for transmission resonance, that θ is an odd multiple of π , is also the condition for a degeneracy of the energy for two consecutive values of the charge on the interfering edge. We now formulate this condition in terms of our energy functional and explore the magnetic field spacings between such resonances.

We start with the integer quantum Hall regime. Let $N_o = n_I + N_L$ be the total number of electrons in the higher Landau levels enclosed by the (almost-closed) interfering edge channel, excluding electrons in the f_T filled Landau levels that correspond to the totally transmitted channels. The energy of the system is then

$$E(N_o, N_L) = \frac{K_I}{2}(N_o - N_L - \phi)^2 + K_{IL}(N_o - N_L - \phi)(N_L + (f_T + 1)\phi - \bar{q}) + \frac{K_L}{2}(N_L + (f_T + 1)\phi - \bar{q})^2 \quad (47)$$

An increase of ϕ by one decreases N_L by $(f_T + 1)$ and increases N_o by f_T . Resonant transmission occurs when there is a vanishing energy cost for adding one electron to the closed edge, that is, a vanishing energy cost for varying N_o by one while keeping N_L fixed. Degeneracy points where N_L changes by ± 1 while N_o is fixed will generally not lead to resonances, even though n_I changes by ∓ 1 at such points. Although the θ will technically pass through an odd multiple of π in this process, one expects that these transitions will generally happen discontinuously, so there is no point at which the resonance could be observed. Points where N_L and N_o increase simultaneously do not involve a change in n_I and do not lead to transmission resonances.

In the extreme AB limit, where $K_{IL} = 0$, there are degeneracy points where $E(N_o, N_L) = E(N_o + 1, N_L + 1)$ separated on the ϕ axis by spacings $\Delta\phi = 1/(f_T + 1)$. These points do not, however, lead to resonances, since they involve a change in N_L . Degeneracy points that do lead to resonances occur when $E(N_o, N_L) = E(N_o + 1, N_L)$, and the spacings between those is $\Delta\phi = 1$, the flux period that characterizes also the weak backscattering regime of the AB limit.

In the extreme CD regime, $K_I = K_{IL}$, and stability requires $K_L > K_I$. Then jumps of N_L are separated from jumps of N_o . In an interval where ϕ increases by 1, there will be f_T resonant events where N_o decreases by one, while N_L is fixed, and $(f_T + 1)$ separate events where N_L increases by one while N_o is fixed. The resonances are thus separated by $\Delta\phi = 1/f_T$. Again, this is the flux period that characterized the CD regime in the weak backscattering limit.

The difference in $\Delta\phi$ between the AB and CD limits characterize also the fractional case. In this case the bulk accommodates N_L quasi-particles of charge e_{in}^* , and the total charge in the ν_{in} region is quantized in units of e_{out}^* . The charge on the interfering edge is given by

$$n_I = N_o e_{out}^* - N_L e_{in}^*. \quad (48)$$

Then, the energy functional becomes,

$$E(N_o, N_L) = \frac{K_I}{2}(e_{out}^* N_o - e_{in}^* N_L - \Delta\nu\phi)^2 + K_{IL}(e_{out}^* N_o - e_{in}^* N_L - \Delta\nu\phi)(e_{in}^* N_L + \nu_{in}\phi - \bar{q}) + \frac{K_L}{2}(e_{in}^* N_L + \nu_{in}\phi - \bar{q})^2 \quad (49)$$

In the Coulomb dominated limit, $K_{IL}/K_I = 1$, and the number of transmission resonances that occur while ϕ changes by one is equal to ν_{out}/e_{out}^* . This leads to $\Delta\phi = e_{out}^*/\nu_{out}$. The leading component in the Fourier transform of $P_R(\phi)$ would then correspond to the $g = 0$ component of (6), just as in the weak backscattering limit.

In the extreme Aharonov-Bohm limit, where $K_{IL} = 0$, the structure of transmission resonances is more complicated, due to the difference between the elementary charges e_{in}^* and e_{out}^* . Just as in the weak backscattering case for the FQHE at $K_{IL} = 0$, there is no single dominant value of g . In the case of weak backscattering, this occurs because $\Delta = 2se_{in}^* \neq 0$, according to Eq. (20). Here we note that $e_{out}^* - e_{in}^* = 2se_{in}^* e_{out}^*$.

Over all, we see that in the limit of strong backscattering, in the CD regime, the number of peaks in the transmission probability as we increase B by one flux quantum is the same number ν_{out}/e_{out}^* as we obtained in the weak backscattering regime, consistent with the prediction that the period of the CD oscillations would not change as we vary r_1 . The strong back scattering limit may also be understood as a Coulomb-Blockade effect: maxima in the transmission probability occur at points where the system consisting of the localized states and the almost-totally-reflected edge state is about to change from one integer value to another.

Typically, the reflection coefficient r_1 should increase from near zero to near unity as one decreases the electron density in the constrictions through the range where the filling factor ν_c at the center of the constriction decreases from slightly below ν_{in} to slightly above ν_{out} . For an ideal constriction, the variation in r_1 should be smooth and monotonic. In real constrictions, however, the variation

may be more complicated, as the Fermi-level may pass through one or more resonances due to tunneling through localized states in the constriction.

Our discussion of the variation in r_1 should also apply if ν_c is varied by changing the magnetic field B rather than by changing a gate voltage at the constriction. Again, the field periods for the AB and CD oscillations should remain fixed as long as $\nu_{\text{out}}/e_{\text{out}}^*$ does not change. However, the parameter Δ which governs the relative strengths of the AB and CD contributions could conceivably change as the other parameters are varied.

Under some circumstances, if there is a large region of intermediate electron density within a constriction, the number of localized states in the constriction may become so large that there is a large density of states at low energies associated with rearrangements of electrons in these states. Then, backscattering through the constriction could become incoherent, either because of inelastic scattering from the low energy modes, or because the path length for tunneling is changed randomly due to thermally excited rearrangements of the localized states. We assume that this does not happen in the system of interest.

VI. MODEL WITH MULTIPLE EDGE STATES

In order to better understand how the presence of multiple edge states may affect the parameters entering the energy function (8), we discuss here some simplified models which may illustrate the physics.

We consider the integer case, with f_T fully transmitted edge states. We define δn_i to be the charge fluctuation associated with a fluctuation in area of the i -th edge state, for $1 \leq i \leq N$, where $N = f_T + 1$, while $\delta n_i = \delta n_L$, for $i = N + 1$. The partially reflected edge state has $i = N$, so $\delta n_I = \delta n_N$.

We may now write the quadratic part of the energy in the form

$$E = \sum_{ij} \frac{\kappa_{ij}}{2} \delta n_i \delta n_j, \quad (50)$$

where the sums go from 1 to $N + 1$. We assume that the coupling constants κ_{ij} are known, and we wish to find the values of the coupling constants K_L, K_I, K_{IL} which entered our earlier computations. We wish to specify the values of δn_L and δn_I , and minimize the energy with respect to the other variables. This means that for $1 \leq j \leq N - 1$, we have

$$\sum_i \kappa_{ji} \delta n_i = 0. \quad (51)$$

The resulting energy will be quadratic in δn_I and δn_L , and the coefficients may be identified with K_I, K_L and K_{IL} .

We illustrate further with two examples. In our first model, we consider a situation where

$$\kappa_{ij} = U + \kappa_1 \delta_{ij}, \quad (52)$$

for $1 \leq i, j \leq N$, and

$$\kappa_{ij} = \kappa_L, \text{ for } i = j = N + 1,$$

$$\kappa_{ij} = V, \text{ if either } i \text{ or } j = N + 1 \text{ but } i \neq j.$$

In this model, the interaction between the edge states is entirely determined by the total edge charge $\sum_{j \leq N} n_j$, and the interaction with N_L involves only that charge. After some straightforward algebra, one obtains the results

$$K_I = \kappa_I + \tilde{U}, \quad K_{IL} = \tilde{V}, \quad (53)$$

where

$$\tilde{U} \equiv U - \frac{f_T U^2}{\kappa_1 + f_T U}, \quad (54)$$

and $\tilde{V} = V \tilde{U} / U$. We see from these results that $K_{IL}/K_I = \tilde{V}/(\kappa_1 + \tilde{U})$. If $V \leq U$ and $f_T > 0$, this ratio is necessarily less than $1/2$, so the model will be in the AB regime. For $f_T = 0$, the model leads to the CD regime if and only if $\kappa_1 + U < 2V$.

The second model we consider is the opposite extreme, where edges are coupled only to their nearest neighbors. We choose the diagonal coupling constants κ_{jj} as the previous model, while for off diagonal couplings we choose $\kappa_{ij} = \kappa_{12}$, if $|i - j| = 1$, and $\kappa_{ij} = 0$ otherwise. Now, we find that coupling to the fully transmitted edges renormalizes the coefficient K_I but has no effect on K_L and K_{IL} , which remain equal to κ_L and κ_{12} , respectively. In the case $f_T = 1$, we find

$$K_I = \kappa_1 - \kappa_{12}^2 / \kappa_1. \quad (55)$$

The value of K_I will be reduced further with increasing f_T , but the value remains finite in the limit of large f_T , where one finds

$$K_I \rightarrow \frac{\kappa_1}{2} + \frac{(\kappa_1^2 - 4\kappa_{12}^2)^{1/2}}{2} \quad (56)$$

We see that in this model, K_I is reduced by up to a factor of 2 as a result of coupling to additional edges. Stability of the model, in the limit of large f_T , requires that $\kappa_{12}/\kappa_1 < 1/2$, and we see that $K_{IL}/K_I < 1$. At the same time, if $2/5 < \kappa_{12}/\kappa_1 < 1/2$, the ratio K_{IL}/K_I will be greater than $1/2$, for sufficiently large f_T , so the system may be pushed from AB into the CD regime. Of course, the CD regime could be reached more easily if the model is modified so that the coupling $\kappa_{N,N+1}$ between the localized charge and the partially reflected edge state is made larger than the other coupling energies, or if the diagonal element κ_{NN} is made smaller than the coefficients κ_{ii} for the fully transmitted edge states.

For a uniform edge of length L , we expect that the constants κ_{ij} should be proportional to $1/L$, for $1 \leq i, j < N$. If we write

$$\kappa_{ij} = \frac{2\pi\hbar}{e^2 L} v_{ij}, \quad (57)$$

then coefficients v_{ij} have the dimensions of velocity. If we can neglect the response of all other degrees of freedom in the system, then fluctuations in the densities δn_i for the edge modes will propagate with velocities that are given by the eigenvalues of the velocity matrix v_{ij} . In actuality, however, the situation is more complicated, as coupling to charges in localized states may reduce the coupling constants κ_{ij} and the propagation velocities by different amounts. The propagation velocities are only affected by rearrangements of charge or polarization that can take place on time scale faster than the time L/v for a pulse to propagate around the interferometer, whereas the constants κ_{ij} entering our formulas are defined for fluctuations on a longer time scale.

VII. CONNECTION TO PREVIOUS THEORETICAL AND EXPERIMENTAL WORKS

Oscillations in the transport properties of quantum Hall devices, associated with interference effects, were already observed in the 1980's, in both IQHE and FQHE regimes.²¹ The possible importance of Coulomb blockade effects²⁹ in these experiments, and of fractional statistics³⁰ for the FQHE situation, was noted by theorists around that time. Interpretation of the early experiments was difficult, however, as the interfering paths were not the result of a deliberate construction but were, presumably, the result of random fluctuations in the doping density, whose geometry was not known. In a typical case, one might see oscillations in the resistance of a micron-scale Hall bar, on the high-field side of a quantized Hall plateau, which might be attributed to backscattering through a “dot” or an “anti-dot” inclusion, where the electron density was higher or lower than in the surrounding electron gas. The strength of tunneling into and out of the dot or anti-dot was generally assumed to be weak, and the oscillations were associated with resonances as additional electrons or quasiparticles were added to the inclusion.³¹ In later years, improved experiments were carried out using fabricated anti-dots with controlled areas, in which one could investigate systematically the dependence on magnetic field and on electron density, controlled by a back gate.³²

Quantum Hall interferometers with the Fabry-Perot geometry studied in the present paper have been explored experimentally by several groups. In several early works, Coulomb blockade effects in a dot *weakly* coupled to leads were studied, in a region with several filled LLs.^{33,34} The crossover between AB and CD regime for a weakly coupled dot was analyzed in [35]. Both integer and fractional quantum Hall interferometers in the absence of charging effects were discussed in [1].

In an earlier experiment³⁶, a strong dependence of the magnetic field period ΔB on the constriction filling factor was found but interpreted in terms of a magnetic field dependent interferometer area. In a reanalysis^{37,38} of that experiment, it was pointed out that under the as-

sumption of a magnetic-field-independent interferometer area, the data agree with $\Delta B \sim 1/\nu_{in}$.

More recently, several groups have conducted systematic investigations of interferometers of different sizes, with and without top gates, in which they could set the filling factor in the constriction independently of the density in the bulk, and data has been collected as a continuous function of both magnetic field and side-gate voltage.^{13,16} The AB regime, the CD regime and the intermediate regime were all observed in these experiments. In the he CD regime, when lines of equal R_D were plotted in the $B - V_G$ plane, they were found to have positive slope for $\nu_{out} \neq 0$, or zero slope for $\nu_{out} = 0$. The CD flux period, in the integer case, was found to be $\Delta\phi = 1/\nu_{out}$, independent of the strength of the backscattering. The AB regime, observed in the IQHE, was characterized by lines of equal R_D that had negative slope in the $B - V_G$ plane and flux periodicity of $\Delta\phi = 1$. Intermediate regimes, where AB and CD behaviors combined together were also observed, giving a checkerboard pattern of the type seen in Fig. [2c].

In the fractional case flux periodicity of $\Delta\phi = 1/\nu_{out}$ was observed in the cases $(\nu_{in}, \nu_{out}) = (\frac{1}{3}, 0)$ and $(\frac{4}{3}, 1)$, where ν_{out} is an integer and ν_{in} a fraction. In the case of $(\frac{2}{5}, \frac{1}{3})$, a period of $\Delta\phi = e_{out}^*/\nu_{out} = 1$ was observed.¹⁶

In an earlier work⁶, in which two of us analyzed the interference patterns in a Fabry-Perot interferometer, a parameter Δ_x/Δ characterizing the strength of bulk-edge coupling was introduced. In the present notation, it corresponds to the ratio K_{IL}/K_I . Here, we have gone beyond the approach of [6] by studying the directions of lines of constant phase and the temperature dependence of the interference terms, and by allowing for arbitrary strength of backscattering.

A first principles approach to the study of interferometers was described in [40]. Possibly due to the approximations chosen in that approach, an influence of Coulomb interactions on the magnetic field period of resistance oscillations was not found.

A situation in which the area of the interfering loop is small compared to the lithographic area, and where it is highly dependent on the magnetic field was discussed in [41]. In this parameter regime, the coefficient λ , defined in our Eq. (42), can be larger than 2, so $(1 - \lambda)^{-1}$ can be negative, with a magnitude smaller than 1. This would cause the Aharonov-Bohm constant-phase lines to have reversed slope, and a period smaller than one flux quantum. However, under this assumption, the magnetic field period would vary continuously, rather than being quantized at a flux quantum divided by an integer, so this mechanism does not seem to explain the experimental findings^{13,16}. Also, this would not explain the simultaneous appearance of AB and CD lines, as observed in several cases.

The influence of anyonic statistics on magnetic field periodicities of Fabry-Perot interferometers was discussed in [39], although the results obtained there disagree in some cases with our findings.

Observations of a magnetic field superperiod, corresponding to an addition of five flux quanta to the interferometer area have been reported in [9,10,42] for a sample in which the bulk is in a quantized Hall state with $\nu = 2/5$, while the constrictions have filling fraction $1/3$. We do not have an explanation for these results. However, we do not accept the theoretical explanation put forth in these papers or in [39]. Although we agree with the arguments which show that addition of five flux quanta should leave the interference pattern unchanged, we believe this should also hold for the addition of a single flux quantum, in the physical model presented in these papers.

VIII. DISCUSSION AND CONCLUSIONS

In this paper, we have presented a general framework for discussing the electronic transport in a quantum Hall Fabry-Perot interferometer. Our aim was to understand the oscillatory dependence of the interferometer resistance R_D on the magnetic field B and voltage applied to a side gate V_G , when these parameters are varied by an amount large enough to change the number of flux quanta or the number of electrons by a finite amount, but small enough so that there is not a large fractional change in either the flux or the electron number. A central assumption was that the resistance arises from the partial reflection of one quantum-Hall edge state in the two constrictions. We also restricted our analysis to the integer quantum Hall states or a subset of fractional states, where all modes at a given edge propagate in the same direction. Our understanding of the physics of the problem was described in general terms in the Introduction, Section I, and in detail in the body of the paper. In this summary we focus on the results we obtained.

We found that δR , the oscillatory part of R_D , is, in general, a two-dimensional periodic function in the plane of B and V_G . It is useful to describe this function in terms of its two-dimensional Fourier transform, which means that we should specify a set of reciprocal lattice vectors \vec{G}_{gh} and the associated amplitudes R_{gh} , where g, h are arbitrary integers, and $\vec{G}_{gh} = g\vec{G}_{10} + h\vec{G}_{01}$. Explicit formulas for the reciprocal lattice basis vectors \vec{G}_{10} and \vec{G}_{01} were given in Subsection III E, in terms of the smoothly varying secular area \bar{A} enclosed by the interfering edge mode, the filling factors ν_{in} and ν_{out} of the quantum Hall states separated by this edge mode, and parameters $\beta, \lambda, \gamma, \eta$ describing the derivatives of \bar{A} and the enclosed “background charge” \bar{q} with respect to V_G and B . Our most general expression for δR is

$$\delta R(B, V_G) = \sum_{gh} R_{gh} e^{i(G_{gh}^{(b)} \delta B + G_{gh}^{(v)} \delta V_G)}, \quad (58)$$

with basis vectors given by (37) and (38). However, in cases where the radius of the interferometer is large compared to the widths of the density transition regions at

the edges, one may be able to neglect the magnetic-field dependence of \bar{A} and \bar{q} , in which case λ and η may be set equal to zero. Then the basis vectors \vec{G}_{10} and \vec{G}_{01} are given by the simpler expressions (33) and (34).

For the remainder of this summary, we shall limit ourselves to the case $\lambda = \eta = 0$. Then, if V_G is held fixed, we find that δR is a periodic function of the magnetic field, with a fundamental period corresponding to the addition of one flux quantum to the area \bar{A} . However, the fundamental period may not have the largest Fourier amplitude, so the most visible oscillations may correspond to a harmonic, with a period that is the fundamental period divided by an integer.

For non-interacting electrons, in the integral quantized Hall effect, the observed interference pattern will reflect the fundamental Aharonov-Bohm period, where the phase increases by 2π when the dimensionless magnetic flux $\phi \equiv B\bar{A}/\phi_0$ changes by one, due to variation of B or of V_G or both. In our current notation, this means that non-zero Fourier components R_{gh} will correspond to reciprocal lattice vectors where $g = h$. In the case of weak backscattering at the constrictions, or at high temperatures, the oscillations are simply sinusoidal, and the dominant contributions are R_{11} and its conjugate $R_{-1,-1}$. On a color-scale map of δR in the $B - V_G$ plane, AB oscillations would appear as a series of parallel stripes with negative slope. For stronger backscattering, at low temperatures, we may get higher Fourier components due to multiple scattering events across the two constrictions.

In the case of weak backscattering, Fourier components at additional reciprocal lattice vectors can arise from electron-electron interactions. For the integer QHE, this is due to the Coulomb interaction between electrons on the interfering edge state and localized electrons or holes which exist in the bulk of the interferometer. Because the number of localized particles is required to be an integer, the net number of localized particles N_L will jump periodically, as B or V_G is varied. Interactions with the edge then cause small variations δA_I in the area A_I enclosed by the interfering edge state, which will cause the actual number of flux quanta enclosed by A_I to fluctuate about the nominal value ϕ , and thus lead to an additional modulation of the interference phase. For FQHE states, there is an additional jump θ_a in the interference phase, arising from the fractional statistics, whenever there is a change in the number of localized quasiparticles.

If the Coulomb coupling between N_L and the edge-state charge is sufficiently strong, one finds that the dominant terms in the Fourier expansion have $g = 0$, both for the IQHE and the FQHE. In this limit, the color-scale map will show a series of stripes which have positive slope and $\Delta\phi = e_{out}^*/\nu_{out}$, except when $\nu_{out} = 0$, in which case the stripes will be horizontal on a $B - V_G$ plot.

In between the AB and CD limits, the two sets of stripes occur simultaneously, and a map of δR will show a checkerboard pattern, as seen in Fig. 2, above. The absolute strengths of the various Fourier coefficients will

depend on the backscattering amplitudes in the individual constrictions and on the temperature, as well as on three energy parameters, which we denote K_I, K_L, K_{IL} . At high temperatures, the Fourier amplitudes will fall off exponentially with T with varying rates, so generally a single pair of Fourier amplitudes will dominate at large T . This may be either the AB term ($g = h = \pm 1$) or the CD term ($g = 0, h = \pm 1$). Then, for a fixed gate voltage, the interference pattern in δR will be a simple sine function of magnetic field, with either the AB or CD period.

At lower temperatures, where many Fourier components maybe present the situation is more complicated. We discuss here the limit of weak backscattering, where h is limited to $h = \pm 1$. Then, at low temperatures, one finds that the phase θ of the interference path is a saw-toothed function of the magnetic field, varying linearly with B most of the time, but with periodic jumps by an amount $2\pi\Delta$, which occur each time the number of localized quasiparticles N_L changes by -1 . There will be ν_{in}/e_{in}^* equally-spaced phase jumps per flux quanta change in the loop, which give rise to Fourier components of $\langle e^{i\theta} \rangle$ with arbitrary values of g . For $h = 1$, at $T = 0$, the Fourier amplitudes vary with g as $(g + \Delta - 1)^{-1}$, according to Eq. (25). At higher temperature the jumps will be smeared, giving a more gradual change of $\langle e^{i\theta} \rangle$ as B is varied. This smearing causes the Fourier amplitudes at the higher g 's to vanish exponentially.

We see from the above that at low temperatures, the AB Fourier amplitude will be larger than the CD amplitude if the jump parameter Δ satisfies $0 < \Delta < 1/2$, while the reverse is true if $1/2 < \Delta < 1$. We find similarly at high temperatures that the AB component will be larger than the CD component if, and only if, $\Delta < 1/2$. For the IQHE Δ is purely a consequence of bulk-edge coupling, and it is equal to K_{IL}/K_I . It vanishes in the extreme AB limit ($K_{IL} \rightarrow 0$) and approaches 1 in the extreme CD limit ($K_{IL} \rightarrow K_I$). For the FQHE, the value of Δ depends on the statistical phase angle θ_a and the ratio K_{IL}/K_I , according to Eq. (20), going from $|\theta_a|/2\pi$, in the absence of bulk-edge coupling, to 1, when this coupling is strong. This suggests the possibility that one could obtain a direct measure of θ_a by observing the discrete jump in the interference phase θ_a as an additional quasihole enters the interferometer at low temperatures. In order to extract the value of θ_a , however, one would have to independently find a measure of K_{IL}/K_I , or be

able to vary K_{IL} (say by varying the area of the interferometer) and extrapolate to $K_{IL} = 0$.

We have said little about the actual values of the parameters β and γ which determine the gate-voltage periods of the AB and CD stripes, nor have we estimated the energy parameters K_I, K_L, K_{IL} , which determine the ratio between the AB and CD amplitudes and the temperature dependence of these amplitudes.

One might try to estimate β and γ using a simplified model, where the electron density in the sample depends on V_G but is independent of B . According to Eq. (11), this means that if one considers a sample with fixed gate voltage, at various values of B , corresponding to different bulk filling factors, the parameter β will be proportional to B , while γ will be independent of B . Using Eq. (34) we find that the V_G period for a CD stripe should be equal to $e_{out}^*/(\gamma - \beta\nu_{out})$. The filling factor ν_{out} will depend on the magnetic field, but also may be varied by changing the voltage on the gates defining the quantum point contact constrictions of the interferometer. It appears that the dependence of the gate period on B and V_G predicted by these considerations is only partly in agreement with experiment, and that significant effects are omitted from this simple model.^{13,16}

Although the energy K_L may be largely determined by the geometric capacitance of the island, the parameters K_{IL} and K_I should be sensitive to the detailed structure of the edge and are difficult to estimate without a detailed microscopic model and a numerical calculation. The values of these parameters should depend also on the value of the magnetic field and on the setting of the constrictions, which determines which edge mode is the interfering one. For a dot of sufficiently large area, covered by a top gate, the parameter K_{IL} should decrease inversely as the area, so for an integer quantized Hall state, one would be necessarily in the AB regime. However, the converse is not true; for a small area dot one could be in the CD or AB regime depending on details. Further investigation of these points will be left for future work.

Acknowledgments: We acknowledge support from NSF grant DMR-0906475, from the Microsoft Corporation, the BSF, the Minerva foundation, and the BMBF. We have benefited from helpful discussions with C.M. Marcus, D. McClure, Y. Zhang, A. Kou, M. Heiblum, N. Ofek, A. Bid, V. Goldman, and R. Willett.

¹ C. de C. Chamon, D.E. Freed, S.A. Kivelson, S.L. Sondhi, and X.G. Wen, Phys. Rev. B **55**, 2331 (1997).

² E. Fradkin, C. Nayak, A. Tsvelik, and F. Wilczek, Nucl. Phys. B **516**, 704 (1998).

³ A. Stern and B.I. Halperin, Phys. Rev. Lett. **96**, 016802 (2006).

⁴ P. Bonderson, A. Kitaev, and K. Shtengel, Phys. Rev. Lett. **96**, 016803 (2006).

⁵ P. Bonderson, K. Shtengel, and J.K. Slingerland, Phys. Rev. Lett. **97**, 016401 (2006).

⁶ B. Rosenow and B.I. Halperin, Phys. Rev. Lett. **98**, 106801 (2007).

⁷ R. Ilan, E. Grosfeld, K. Schoutens, and A. Stern, Phys. Rev. B **79**, 245305 (2009).

⁸ Y. Ji, Y. Chung, D. Sprinzak, M. Heiblum, D. Mahalu, and H. Shtrikman, Nature **422**, 415 (2003).

- ⁹ F.E. Camino, Wei Zhou, and V.J. Goldman, Phys. Rev. Lett. **95**, 246802 (2005).
- ¹⁰ F.E. Camino, Wei Zhou, and V.J. Goldman, Phys. Rev. B **76**, 155305 (2007).
- ¹¹ F.E. Camino, Wei Zhou, and V.J. Goldman, Phys. Rev. Lett. **98**, 076805 (2007).
- ¹² M.D. Godfrey, P. Jiang, W. Kang, S. H. Simon, K.W. Baldwin, L.N. Pfeiffer, and K.W. West, preprint arXiv:0708.2448 (2007).
- ¹³ Y. Zhang, D.T. McClure, E.M. Levenson-Falk, C.M. Marcus, L.N. Pfeiffer, and K.W. West, Phys. Rev. B **79**, 241304 (2009).
- ¹⁴ D.T. McClure, Y. Zhang, B. Rosenow, E.M. Levenson-Falk, C.M. Marcus, L.N. Pfeiffer, and K.W. West, Phys. Rev. Lett. **103**, 206806 (2009).
- ¹⁵ Ping V. Lin, F.E. Camino, and V.J. Goldman, Phys. Rev. B **80**, 125310 (2009).
- ¹⁶ N. Ofek, A. Bid, M. Heiblum, A. Stern, V. Umansky, D. Mahalu, preprint arXiv:0911.0794 (2009).
- ¹⁷ R.L. Willett, L.N. Pfeiffer, and K.W. West, PNAS **0812599106** (2009).
- ¹⁸ R.L. Willett, L.N. Pfeiffer, and K.W. West, preprint arXiv:0911.0345 (2009).
- ¹⁹ B.W. Alphenaar, A.A.M. Staring, H. van Houten, M.A.A. Mabeoone, O.J.A. Buyk, and C.T. Foxon, Phys. Rev. B **46**, 7236 (1992).
- ²⁰ S. Ilani, J. Martin, E. Teitelbaum, J.H. Smet, D. Mahalu, V. Umansky, and A. Yacoby, Nature **427**, 328 (2004).
- ²¹ See, *e.g.*, J. A. Simmons, H. P. Wei, L. W. Engel, D. C. Tsui, and M. Shayegan, Phys. Rev. Lett. **63**, 1731 (1989); and references therein.
- ²² B. Hackens, F. Martins, S. Faniel, C.A. Dutu, H. Sellier, S. Huant, M. Pala, L. Desplanque, X. Wallart, and V. Bayot, Nature Commun. **1**, 39 (2010).
- ²³ C.W.J. Beenakker and H. van Houten in: H. Ehrenreich and D. Turnbull, Editors, Solid State Physics **44**, Academic Press, New York (1992), p. 1.
- ²⁴ A. K. Evans, L. I. Glazman, and B. I. Shklovskii, Phys. Rev. B **48**, 11120 (1993).
- ²⁵ B. I. Halperin, Phys. Rev. Lett. **52**, 1583 (1984).
- ²⁶ B. Blok and X. G. Wen, Phys. Rev. B **42**, 8145 (1990).
- ²⁷ Ady Stern, Annals of Physics **323**, 204 (2008).
- ²⁸ X. G. Wen, Phys. Rev. B **44**, 5708 (1991).
- ²⁹ P.A. Lee, Phys. Rev. Lett. **65**, 2206 (1990).
- ³⁰ S. Kivelson, Phys. Rev. Lett. **65**, 3369 (1990).
- ³¹ J.K. Jain and S. Kivelson, Phys. Rev. Lett. **60**, 1542 (1988).
- ³² V.J. Goldman and B. Su, Science **267**, 1010 (1995).
- ³³ P.L. McEuen, E.B. Foxman, Jari Kinaret, U. Meirav, M.A. Kastner, Ned S. Wingreen, and S.J. Wind, Phys. Rev. B **45**, 11419 (1992).
- ³⁴ C.M. Marcus, A.J. Rimberg, R.M. Westervelt, P.F. Hopkins, and A.C. Gossard, Surf. Science **305**, 480 (1994).
- ³⁵ C.W.J. Beenakker, H. van Houten, and A.A.M. Staring, Phys. Rev. B **44**, 1657.
- ³⁶ B.J. van Wees, L.P. Kouwenhoven, C.J.P.M. Harmans, J.G. Williamson, C.E. Timmering, M.E.I. Broekaart, C.T. Foxon, and J.J. Harris, Phys. Rev. Lett. **62**, 2523 (1989).
- ³⁷ F.E. Camino, W. Zhou, and V.J. Goldman, Phys. Rev. B **72**, 155313 (2005).
- ³⁸ M.W.C. Dharma-wardana, R.P. Taylor, and A.S. Sachrajda, Solid State Commun. **84**, 631 (1992).
- ³⁹ V.J. Goldman, Phys. Rev. B **75**, 045334 (2007).
- ⁴⁰ S. Ihnatsenka and I.V. Zozoulenko, Phys. Rev. B **77**, 235304 (2008).
- ⁴¹ A. Siddiki, preprint arXiv:1006.5012 (2010).
- ⁴² V. L. Ping, F. E. Camino, and V. J. Goldman, Phys. Rev. B **80**, 235301 (2009).